THE JOURNAL OF PHYSICAL CHEMISTRY Letters

Letter

pubs.acs.org/JPCL

Multiexciton Solar Cells of $CuInSe_2$ Nanocrystals

C. Jackson Stolle,[†] Taylor B. Harvey,[†] Douglas R. Pernik,[†] Jarett I. Hibbert,[†] Jiang Du,[†] Dong Joon Rhee,[†] Vahid A. Akhavan,[‡] Richard D. Schaller,[§,∥] and Brian A. Korgel*[,†]

[†]McKetta Department of Chemical Engineering, Texas Materials Institute, Center for Nano- and Molecular Science and Technology, The University of Texas at Austin, Austin, Texas 78712, United States

[‡]NovaCentrix, 200-B Parker Drive, Suite 580, Austin, Texas 78728, United States

[§]Center for Nanoscale Materials, Argonne National Laboratories, Argonne, Illinios 60439, United States

[∥]Department of Chemistry, Northwestern University, Evanston, Illinois 60208, United States

S *Supporting Information*

ABSTRACT: Peak external quantum efficiencies (EQEs) of just over 120% were observed in photovoltaic (PV) devices of $CuInSe_2$ nanocrystals prepared with a photonic curing process. The extraction of more than one electron/hole pair as a result of the absorption of a single photon can occur if multiple excitons are generated and extracted. Multiexciton generation (MEG) in the nanocrystal films was substantiated by transient absorption spectroscopy. We propose that photonic curing leads to sufficient electronic coupling between nanocrystals to enable multiexciton extraction under typical solar illumination conditions. Under low light conditions, however, the EQE drops significantly, indicating that photonic curing-induced ligand desorption creates a significant amount of traps in the film that limit the overall power conversion efficiency of the device.

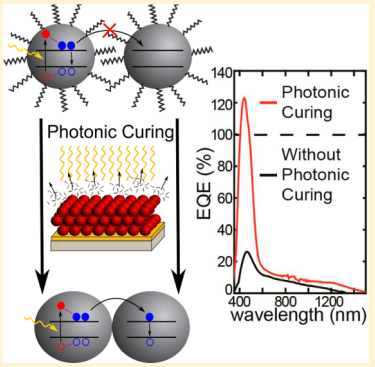

SECTION: Physical Processes in Nanomaterials and Nanostructures

A maximum of 34% of the energy available in sunlight can be converted to electricity by a single junction solar cell, known as the Shockley–Queisser limit.[1] The semiconductor in the device does not absorb photons with energy less than its band gap energy, and photon energy greater than the band gap is lost as heat due to the rapid relaxation of the photoexcited electron and hole to their band minima before they can be extracted as electrical current. One way to surpass the Shockley–Queisser limit is to use quantum dots that convert high-energy photons into multiple electron–hole pairs that can be extracted as photocurrent by the device.[2,3] Colloidal nanocrystals provide a convenient source of quantum dots in which multiexciton generation (MEG) has been observed optically from a host of materials, including PbS, PbSe, PbTe, CdSe, InAs, and Si.[4−8] Extraction of more than one electron per absorbed photon as electrical current in devices has also been reported,[9−12] with a few instances of device quantum efficiencies (QEs) exceeding 100%, PbS (internal QE only),[13] PbSe (external QE, EQE)[14] nanocrystal solar cells, and an organic device exhibiting a related process of singlet fission.[15] Here, we report photovoltaic (PV) devices of $CuInSe_2$ nanocrystals with peak EQEs of over 120% that result from multiexciton generation and extraction.

$CuInSe_2$ is an important model semiconductor for PV devices that is closely related to $Cu(In_xGa_{1-x})Se_2$ (CIGS), which holds the record for highest device efficiency of all thin film semiconductors at just over 20%.[16] PV devices made from ink-deposited $CuInSe_2$ nanocrystals have reached power conversion efficiencies of 3%, limited by poor charge transport.[17−19] Ink-deposited $Cu(In_xGa_{1-x})S_2$ nanocrystals can be sintered into polycrystalline films by heating (>500 °C) under selenium vapor (i.e., selenization) to achieve much higher efficiencies of just over 12%.[20,21] To try to avoid the need for high temperature selenization, an alternative nanocrystal film processing technique called photonic curing is explored here to improve charge transport in the nanocrystal film. Photonic curing was carried out using a PulseForge 3300 (NovaCentrix) tool that uses pulsed light from a xenon flash lamp with spectrally broad blackbody radiation that can rapidly heat to very high temperature. Photonic curing can provide enough energy to sinter nanocrystals,[22] but in this study, relatively mild pulse conditions were used to remove organic ligands and bring nanocrystals into better electrical contact without destroying their nanoscale dimensions. Nanocrystal films processed in this way were found to yield PVs with peak EQEs exceeding 100%, indicating the possible occurrence of MEG and extraction from the devices. Transient absorption (TA) spectroscopy was employed to verify that MEG does indeed occur in the nanocrystal films.

Received: November 29, 2013
Accepted: December 26, 2013
Published: December 26, 2013

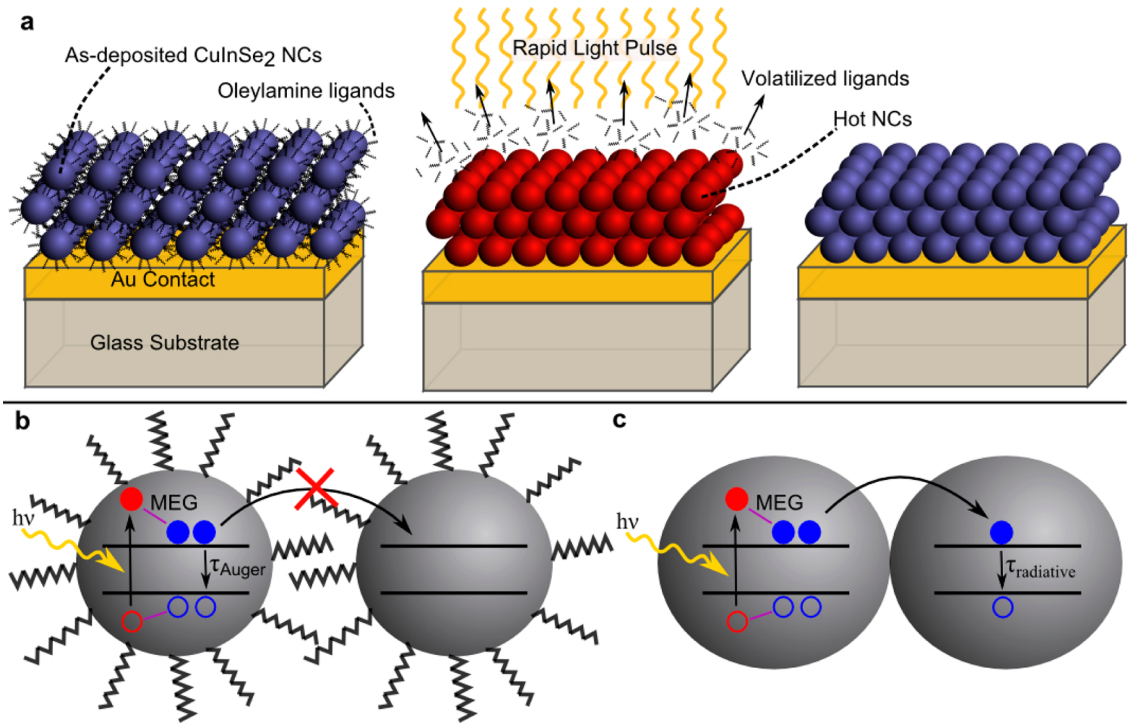

Figure 1. Photonic curing of nanocrystal films on Au-coated glass substrates. (a) Photonic curing can be used to remove oleylamine capping ligands from the $CuInSe_2$ nanocrystal film without inducing nanocrystal grain growth. (b) When the capping ligands are present, they inhibit the collection of multiexcitons from the film, leading to electron–hole recombination by Auger recombination. (c) Without the ligand barrier between nanocrystals, multiexciton transport becomes much more probable.

PV devices were made by spray-depositing $CuInSe_2$ nanocrystals from toluene dispersions on Au-coated soda lime glass substrates similar to Akhavan et al.[17] and then curing the nanocrystal films with the PulseForge tool (Figure 1) in a closed chamber with a quartz window using a single 160 μs light pulse with flux ranging from 2 to 3 J/cm^2. The CdS buffer layer and ZnO/ITO top contacts were then added. Nanocrystal films pulsed with 2.2 J/cm^2 light reach about 600 °C within 1 ms, which removes the oleylamine ligand but does not induce crystal grain growth (see Supporting Information Figures S1–S5). Figure 2 shows scanning electron microscope (SEM) images of $CuInSe_2$ nanocrystal films before and after curing with 2.2 and >3 J/cm^2 exposure. The nanocrystal grains remain small after 2.2 J/cm^2 exposure but clearly grow into larger grains after >3 J/cm^2 exposure. (See also the X-ray diffraction (XRD) peak width data in Figure S4 in the Supporting Information)

Although the nanocrystals could be grown into large grains by photonic curing, devices made from these sintered nanocrystals performed very poorly, as shown in Figure 2. Exposure of 3 J/cm^2 sintered the nanocrystals but also led to dewetting by the formation of melt balls, leaving significant back contact exposed and devices with almost no short-circuit current. In contrast, devices made with nanocrystals cured using 2.2 J/cm^2 exposure gave reasonable device response with a power conversion efficiency (PCE) of 1.25%, similar to the devices made with as-deposited nanocrystals (PCE = 1.19%). The biggest change in device response after photonic curing is a large increase in the short-ci,rcuit current (J_{sc}) and a drop in the open-circuit voltage (V_{oc}); for example, in Figure 2g the J_{sc} and V_{oc} changed from 5.65 to 18.65 mA/cm^2 and 0.41 to 0.21 V, respectively.

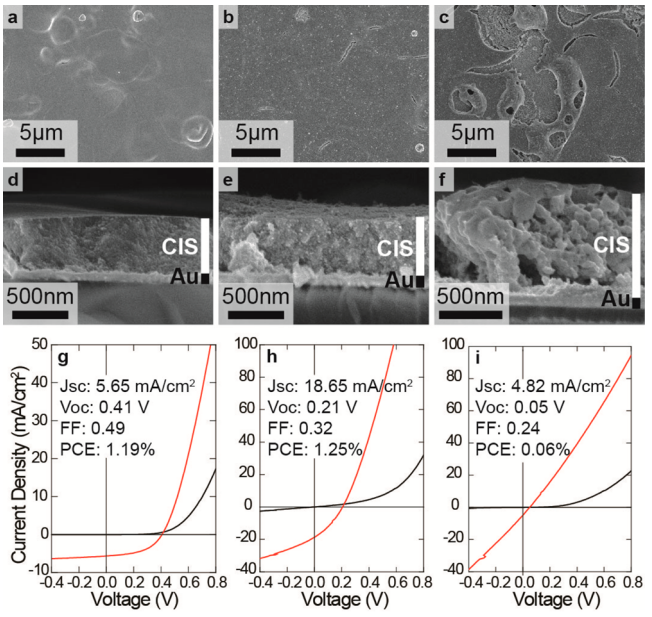

Figure 2. $CuInSe_2$ nanocrystal layers before and after photonic curing and their PV device performance. Top-down and cross-sectional SEM images of an oleylamine-capped $CuInSe_2$ (CIS) nanocrystal film on Au-coated glass (a, d) before and after photonic curing with (b, e) 2.2 and (c, f) and 3 J/cm^2 pulse fluence. (g–i) Corresponding current–voltage measurements (the black curve is dark current; the red curve is measured under AM1.5G illumination (100 mW/cm^2)) of devices made with the nanocrystal films provided below the SEM images.

EQE (also known as IPCE) measurements showed that most of the increased short-circuit current in the devices made with cured nanocrystals occurred in the short wavelength (<600

dx.doi.org/10.1021/jz402596v | J. Phys. Chem. Lett. 2014, 5, 304–309

nm) range. Figure 3a shows a comparison of EQE spectra from PVs made with as-deposited $CuInSe_2$ nanocrystals and

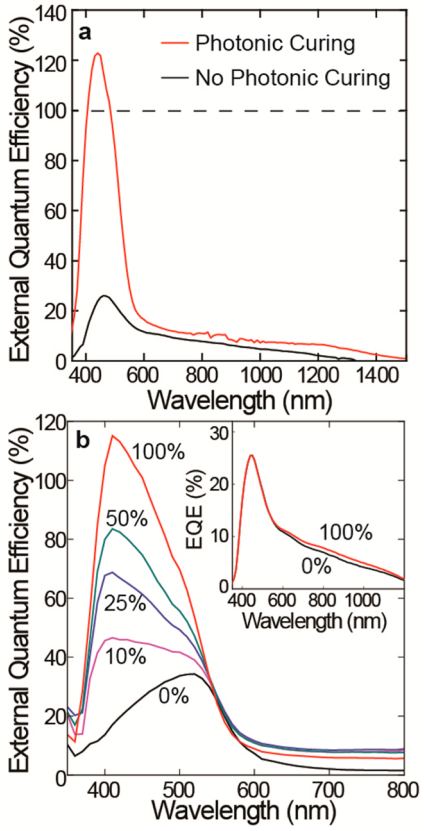

Figure 3. EQE enhancements resulting from photonic curing of the $CuInSe_2$ nanocrystal layer used in PV devices. (a) EQE measurements taken under white light bias (50 mW/cm^2) for $CuInSe_2$ nanocrystal devices without photonic curing (black curve) compared to the device made with cured (2.2 J/cm^2 pulse fluence) nanocrystals (red curve). The short-circuit currents determined from these data, of 4.95 and 14.29 mA/cm^2, are consistent with the short-circuit currents measured under AM1.5 illumination (100 mW/cm^2). (b) EQE measured under varying white light bias intensity (100, 50, 25, 10, and 0% of a 50 mW/cm^2 bias light) with the same intensity of monochromated probe light. There was no change in EQE for the device made with as-deposited nanocrystals (inset), but the EQE decreased significantly for the cured device when the white light bias intensity was reduced to the amounts indicated.

nanocrystals that had been processed by photonic curing at 2.2 J/cm^2. The measurements in Figure 3a are made under a white light bias of 50 mW/cm^2. The as-deposited $CuInSe_2$ nanocrystal device has a peak EQE of about 25%, whereas the peak EQE of the cured nanocrystal device is 123%. On the basis of the measured light absorption in the device, the peak internal quantum efficiency (IQE) was found to correspond to 143% (Supporting Information Figure S6). The application of a white light bias has little effect on the as-deposited $CuInSe_2$ nanocrystal devices but had a significant influence on the EQE spectra of the cured nanocrystal devices (see Figure 3b, for example).

The substantial effect of white light bias on the EQE of cured nanocrystal devices indicates that the curing process introduces traps into the nanocrystal layer that hinder charge extraction under low light conditions.[25,26] Because EQE measurements of solar cells are performed with a low-intensity monochromatic probe beam, the additional intense white light bias is required to mimic the near full sun conditions experienced by the device in the field,[23] and EQE measurements taken without white light bias can give anomalous results.[23−26] For example, traps in the CdS layer in CdTe/CdS devices usually filled under AM1.5 illumination remain empty under low light conditions, significantly reducing device currents and leading to artificially low EQE values if white light bias is not used.[23−26] CdTe and CIGS PV devices can also exhibit EQE variations with light bias intensity due to photoconductive CdS.[24−27] In our case, the CdS layer is the same for all devices, and the EQE of the as-deposited nanocrystal device is not affected by the white light bias intensity (Figure 3b, inset). However, most telling is that the EQE of the devices with peak EQE > 100% was found to decrease proportionally with the probe light intensity (Supporting Information Figure S7, Table S1), additionally ruling out possible contributions from photoconductive gain or anomalous currents due to trapped carrier extraction related to the bias illumination. The EQE also did not vary with probe beam chopping frequency (Supporting Information Figure S8), eliminating the likelihood of measurement artifacts due to slow carrier kinetics. Lastly, the measured J_{sc} values of the $CuInSe_2$ nanocrystal devices in Figure 2 agree pretty well with those calculated from the EQE measurements in Figure 3. The measured J_{sc} from the as-deposited nanocrystal device was 5.65 mA/cm^2, compared to 4.95 mA/cm^2 calculated from EQE data. The cured nanocrystal device J_{sc} is 18.65 mA/cm^2 (Figure 2h), compared to 14.29 mA/cm^2 calculated from the EQE data. The lower calculated J_{sc} value for the cured nanocrystal device results from the fact that the white light bias intensity in our IPCE setup was limited to ∼50 mW/cm^2, and because the EQE of these devices was sensitive to the bias intensity, the measured EQE under white light bias was still slightly lower than that under true AM1.5 illumination at 100 mW/cm^2.

To help verify that MEG occurs in the nanocrystal films that exhibit peak EQE > 100%, the recombination dynamics of photoexcited excitons were determined by TA spectroscopy with 400 and 800 nm pump light. Figure 4a,b shows the decay in bleach signal near the absorption edge (see Supporting Information Figure S9 for a spectrum of the bleach signal).[28,29] Multiexcitons undergo Auger recombination (the inverse process to MEG) on very short time scales (typically ∼100 ps) compared to much longer lived single excitons.[28] With 800 nm pump light (Figure 4a), an individual photon does not have enough energy to induce MEG, and only one exciton per nanocrystal is generated at low pump fluence. Under these conditions, the kinetics curves (normalized at delay times >1 ns) overlap. When the 800 nm pump fluence is increased so that some nanocrystals absorb more than one photon per excitation pulse, multiexcitons form and Auger recombination dynamics arise. The 400 nm pump photons carry about three times the band gap energy; therefore, MEG from a single photon is possible, and Auger recombination dynamics can be observed even at low fluences. Figure 4b shows the bleach signal for two low-fluence TA kinetics with 400 nm pump wavelength as well as an average of the 3, 6, and 15 μJ/cm^2 TA curves at 800 nm pump wavelength for comparison. The low-fluence TA kinetics at 400 nm show increased signal at short times compared to the low-fluence 800 nm pump TA kinetics, indicating the presence of Auger recombination and therefore MEG. The possibility of anomalous results due to photocharging was eliminated by rapidly translating the sample through the measurement area.[30] Negligible differences were

dx.doi.org/10.1021/jz402596v | J. Phys. Chem. Lett. 2014, 5, 304−309

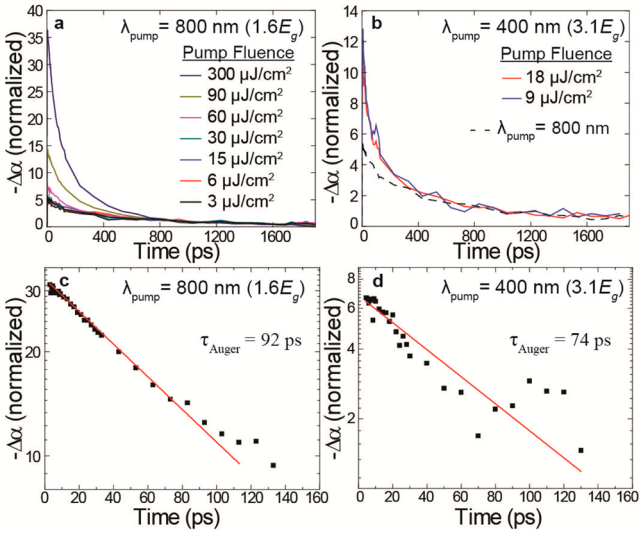

Figure 4. TA spectroscopy of $CuInSe_2$ nanocrystal films after photonic curing. (a) TA kinetics normalized to $-\Delta\alpha = 1$ at 1000 ps with an 800 nm pump wavelength and pump fluences of 300 (dark blue), 90 (green), 60 (pink), 30 (teal), 15 (blue), 6 (red), and 3 $\mu J/cm^2$ (black). (b) TA kinetics normalized to $-\Delta\alpha = 1$ at 1000 ps with a 400 nm pump wavelength and pump fluences of 18 (red) and 9 $\mu J/cm^2$ (blue). The average low fluence background (average of 3, 6, 15, and 30 $\mu J/cm^2$ signals) at an 800 nm pump wavelength is also shown for comparison (black). (c) TA kinetics showing the Auger recombination rate. The single exciton TA kinetics background (average 800 nm wavelength low-fluence pump) is subtracted from the high-fluence TA kinetics at an 800 nm, 300 $\mu J/cm^2$ pump, which shows the creation of multiexcitons due to the absorption of multiple photons per nanocrystal. The kinetics are plotted on a log scale and can be fitted to a single exponential with a time constant of 92 ps. (d) TA kinetics showing Auger recombination at a 400 nm pump and low fluence. The single-exciton TA kinetics background (average 800 nm wavelength low-fluence pump) is subtracted from the TA kinetics at a 400 nm, 9 $\mu J/cm^2$ pump, which should only show Auger recombination if MEG is present. The kinetics are plotted on a log scale and can be fitted to a single exponential with a time constant of 74 ps.

observed between measurements of static and translating samples (Supporting Information Figure S10).

The average single exciton recombination kinetics at an 800 nm pump and low fluence was used as a baseline to determine the Auger recombination rate. In Figure 4c,d, the single-exciton recombination background kinetics were subtracted (time constant of ~600 ps) from the TA kinetics at the 800 nm pump wavelength and 300 $\mu J/cm^2$ fluence (a high-power regime where multiple photons are present per absorbing nanocrystal) and at the 400 nm pump wavelength and 9 $\mu J/cm^2$ fluence (in the regime of less than one photon per nanocrystal). The curves in Figure 4c,d both fit single exponentials with similar time constants of 93 and 74 ps, respectively. The presence of Auger recombination at low fluences of 400 nm pump light supports the presence of MEG in the cured $CuInSe_2$ nanocrystal films, and the estimated MEG quantum yield of 125% is close to the device peak IQE measurements of ~143% (see Supporting Information Figures S6 and S11).

The influence of the trap states limiting multiexciton extraction under low light conditions on the exciton decay dynamics was tested by applying an intense white light bias during TA measurements, and there was little effect on the TA kinetics (see Supporting Information Figure S12). The traps seem to have a detrimental effect only on charge extraction. Perhaps these traps are related to unpassivated surface defects.[31−34] TEM shows that prior to photonic curing, the nanocrystals have a diameter of 8.1 ± 2.1 nm, which is smaller than the Bohr exciton radius for $CuInSe_2$ (Supporting Information Figure S5).[35] The red shift of 60 meV in the peak wavelength of the absorption bleach in the TA spectrum (Supporting Information Figure S9) after curing is consistent with a slight loss of quantum confinement resulting from the loss of capping ligands. However, the fact that the reduction in optical gap is larger than this (0.12 eV, Supporting Information Figure S13) and that the TA spectrum exhibits an asymmetric broadening into the red part of the spectrum (Supporting Information Figure S9) indicate that trap-related defects are present after photonic curing. In order to extract multiexcitons from a device, the photogenerated multiple electron−hole pairs must separate before Auger recombination can occur. CdTe and PbS nanocrystals both show charge-transfer rates between nanocrystals of ~100 ps, and biexcitons can be extracted from separate nanocrystals prior to Auger recombination.[9,36−38] Charge transfer rates as fast as 50 fs have been observed in PbSe nanocrystals and reported as hot carrier extraction.[39] Our calculated biexciton decay time is similar to that of coupled PbSe quantum dot films (~100 ps), which have also demonstrated MEG in devices.[14,28] Enhanced coupling in films of PbSe nanocrystals has enabled efficient conversion of multiexcitons into free charge carriers compared to the competing Auger recombination process.[40] In films of $CuInSe_2$ nanocrystals coated with oleylamine ligands, charge carrier separation is inefficient, and multiexcitons are lost to Auger recombination (see Figure 1b). The observation of peak QEs over 100% after photonic curing indicates that multiexciton dissociation and extraction (as individual charges or as excitons) becomes much more efficient (see Figure 1c).

Ink-deposited $CuInSe_2$ nanocrystal PVs treated by photonic curing exhibited high short-circuit currents and peak EQEs of over 120%. TA measurements provide substantiation that the high EQE results from the extraction of multiexcitons. It appears that photonic curing brings the nanocrystals into better electrical contact and enables multiexciton extraction. Ligand removal, however, also seems to induce a significant amount of traps in the nanocrystal film, which reduces device performance, especially under low light conditions. Passivation of these surface traps could perhaps provide a route to high-efficiency devices that utilize MEG and extraction along with reasonably efficient charge extraction for electrons and holes photoexcited closer to the band gap energy.

■ ASSOCIATED CONTENT

Supporting Information

Experimental details, including materials used, nanocrystal synthesis, film deposition methods, PV device fabrication, characterization, and PV device testing, additional data ans supplementary figures, including the confirmation of ligand loss during photonic curing of nanocrystal films by TGA and FTIR, the calculated substrate temperature during photonic curing process, the extent of nanocrystal sintering after photonic curing determined by XRD, the IQE and MEG quantum yields, the effect of light biasing on EQE measurements, and TA spectroscopy, and Table S1, showing the EQE and calculated J_{sc} for each probe beam intensity. This material is available free of charge via the Internet at http://pubs.acs.org.

dx.doi.org/10.1021/jz402596v | J. Phys. Chem. Lett. 2014, 5, 304−309

AUTHOR INFORMATION

Corresponding Author

*E-mail: korgel@che.utexas.edu. Tel.: +1-512-471-5633. Fax: +1-512-471-7060.

Notes

The authors declare no competing financial interest.

ACKNOWLEDGMENTS

Financial support of this work was provided by the Robert A. Welch Foundation (F-1464) and the National Science Foundation Industry/University Cooperative Research Center on Next Generation Photovoltaics (IIP-1134849). Financial support was also provided for C.J.S. and D.R.P. by the National Science Foundation Graduate Research Fellowship program under Grant No. DGE-1110007. Use of the Center for Nanoscale Materials was supported by the U. S. Department of Energy, Office of Science, Office of Basic Energy Sciences, under Contract No. DE-AC02-06CH11357. The authors also thank Sayan Saha and Sanjay Banerjee for use of their QEX10 Solar Cell Spectral Response Measurement System.

REFERENCES

(1) Henry, C. H. Limiting Efficiencies of Ideal Single and Multiple Energy Gap Terrestrial Solar Cells. *J. Appl. Phys.* **1980**, *51*, 4494−4500.
(2) Hanna, M. C.; Nozik, A. J. Solar Conversion Efficiency of Photovoltaic and Photoelectrolysis Cells with Carrier Multiplication Absorbers. *J. Appl. Phys.* **2006**, *100*, 074510.
(3) Beard, M. C. Multiple Exciton Generation in Semiconductor Quantum Dots. *J. Phys. Chem. Lett.* **2011**, *2*, 1282−1288.
(4) Schaller, R. D.; Klimov, V. I. High Efficiency Carrier Multiplication in PbSe Nanocrystals: Implications for Solar Energy Conversion. *Phys. Rev. Lett.* **2004**, *92*, 186601.
(5) Beard, M. C.; Knutsen, K. P.; Yu, P.; Luther, J. M.; Song, Q.; Metzger, W. K.; Ellingson, R. J.; Nozik, A. J. Multiple Exciton Generation in Colloidal Silicon Nanocrystals. *Nano Lett.* **2007**, *7*, 2506−2512.
(6) Murphy, J. E.; Beard, M. C.; Norman, A. G.; Ahrenkiel, S. P.; Johnson, J. C.; Yu, P.; Mićić, O. I.; Ellingson, R. J.; Nozik, A. J. PbTe Colloidal Nanocrystals: Synthesis, Characterization, and Multiple Exciton Generation. *J. Am. Chem. Soc.* **2006**, *128*, 3241−3247.
(7) Lin, Z.; Franceschetti, A.; Lusk, M. T. Size Dependence of the Multiple Exciton Generation Rate in CdSe Quantum Dots. *ACS Nano* **2011**, *5*, 2503−2511.
(8) Califano, M. Direct and Inverse Auger Processes in InAs Nanocrystals: Can the Decay Signature of a Trion Be Mistaken for Carrier Multiplication? *ACS Nano* **2009**, *3*, 2706−2714.
(9) Sukhovatkin, V.; Hinds, S.; Brzozowski, L.; Sargent, E. H. Colloidal Quantum-Dot Photodetectors Exploiting Multiexciton Generation. *Science* **2009**, *324*, 1542−1544.
(10) Kim, S. J.; Kim, W. J.; Sahoo, Y.; Cartwright, A. N.; Prasad, P. N. Multiple Exciton Generation and Electrical Extraction from a PbSe Quantum Dot Photoconductor. *Appl. Phys. Lett.* **2008**, *92*, 031107/1−031107/3.
(11) Kim, S. J.; Kim, W. J.; Cartwright, A. N.; Prasad, P. N. Carrier Multiplication in a PbSe Nanocrystal and P3HT/PCBM Tandem Cell. *Appl. Phys. Lett.* **2008**, *92*, 191107/1−191107/3.
(12) Gabor, N. M.; Zhong, Z.; Bosnick, K.; Park, J.; McEuen, P. L. Extremely Efficient Multiple Electron−Hole Pair Generation in Carbon Nanotube Photodiodes. *Science* **2009**, *325*, 1367−1371.
(13) Sambur, J. B.; Novet, T.; Parkinson, B. A. Multiple Exciton Collection in a Sensitized Photovoltaic System. *Science* **2010**, *330*, 63−66.
(14) Semonin, O. E.; Luther, J. M.; Choi, S.; Chen, H.-Y.; Gao, J.; Nozik, A. J.; Beard, M. C. Peak External Photocurrent Quantum Efficiency Exceeding 100% via MEG in a Quantum Dot Solar Cell. *Science* **2011**, *334*, 1530−1533.
(15) Congreve, D. N.; Lee, J.; Thompson, N. J.; Hontz, E.; Yost, S. R.; Reusswig, P. D.; Bahlke, M. E.; Reineke, S.; Voorhis, T. V.; Baldo, M. A. External Quantum Efficiency Above 100% in a Singlet-Exciton-Fission-Based Organic Photovoltaic Cell. *Science* **2013**, *340*, 334−337.
(16) Jackson, P.; Hariskos, D.; Lotter, E.; Paetel, S.; Wuerz, R.; Menner, R.; Wischmann, W.; Powalla, M. New World Record Efficiency for Cu(In,Ga)Se_2 Thin-Film Solar Cells Beyond 20%. *Prog. Photovoltaics Res. Appl.* **2011**, *19*, 894−897.
(17) Akhavan, V. A.; Panthani, M. G.; Goodfellow, B. W.; Reid, D. K.; Korgel, B. A. Thickness-Limited Performance of $CuInSe_2$ Nanocrystal Photovoltaic Devices. *Opt. Express* **2010**, *18*, A411−A420.
(18) Stolle, C. J.; Panthani, M. G.; Harvey, T. B.; Akhavan, V. A.; Korgel, B. A. Comparison of the Photovoltaic Response of Oleylamine and Inorganic Ligand-Capped $CuInSe_2$ Nanocrystals. *ACS Appl. Mater. Interfaces* **2012**, *4*, 2757−2761.
(19) Panthani, M. G.; Stolle, C. J.; Reid, D. K.; Rhee, D. J.; Harvey, T. B.; Akhavan, V. A.; Yu, Y.; Korgel, B. A. $CuInSe_2$ Quantum Dot Solar Cells with High Open-Circuit Voltage. *J. Phys. Chem. Lett.* **2013**, *4*, 2030−2034.
(20) Guo, Q.; Ford, G. M.; Agrawal, R.; Hillhouse, H. W. Ink Formulation and Low-Temperature Incorporation of Sodium to Yield 12% Efficient Cu(In,Ga)$(S,Se)_2$ Solar Cells from Sulfide Nanocrystal Inks. *Prog. Photovoltaics Res. Appl.* **2012**, *21*, 64−71.
(21) Akhavan, V. A.; Harvey, T. B.; Stolle, C. J.; Ostrowski, D. P.; Glaz, M. S.; Goodfellow, B. W.; Panthani, M. G.; Reid, D. K.; Vanden Bout, D. A.; Korgel, B. A. Influence of Composition on the Performance of Sintered Cu(In,Ga)Se_2 Nanocrystal Thin-Film Photovoltaic Devices. *ChemSusChem* **2013**, *6*, 481−486.
(22) Schroder, K. A. Mechanisms of Photonic Curing: Processing High Temperatures on Low Temperature Substrates. *Nanotech Conf. Expo 2011* **2011**, *2*, 220−223.
(23) Sites, J. R.; Tavakolian, H.; Sasala, R. A. Analysis of Apparent Quantum Efficiency. *Sol. Cells* **1990**, *29*, 39−48.
(24) Hegedus, S. S. The Photoresponse of CdS/$CuInSe_2$ Thin-Film Heterojunction Solar Cells. *IEEE Trans. Electron Devices* **1984**, *31*, 629−633.
(25) Hegedus, S.; Ryan, D.; Dobson, K.; McCandless, B.; Desai, D. Photoconductive CdS: How Does It Affect CdTe/CdS Solar Cell Performance? *MRS Online Proc. Libr.* **2003**, *763*, B9.5.1−B9.5.6.
(26) Gloeckler, M.; Sites, J. R. Apparent Quantum Efficiency Effects in CdTe Solar Cells. *J. Appl. Phys.* **2004**, *95*, 4438−4445.
(27) Demtsu, S.; Albin, D.; Sites, J. Role of Copper in the Performance of CdS/CdTe Solar Cells. In *Conference Record of the 2006 IEEE 4th World Conference on Photovoltaic Energy Conversion*; 2006; Vol. *1*, pp 523−526.
(28) Luther, J. M.; Beard, M. C.; Song, Q.; Law, M.; Ellingson, R. J.; Nozik, A. J. Multiple Exciton Generation in Films of Electronically Coupled PbSe Quantum Dots. *Nano Lett.* **2007**, *7*, 1779−1784.
(29) Stewart, J. T.; Padilha, L. A.; Qazilbash, M. M.; Pietryga, J. M.; Midgett, A. G.; Luther, J. M.; Beard, M. C.; Nozik, A. J.; Klimov, V. I. Comparison of Carrier Multiplication Yields in PbS and PbSe Nanocrystals: The Role of Competing Energy-Loss Processes. *Nano Lett.* **2012**, *12*, 622−628.
(30) McGuire, J. A.; Sykora, M.; Joo, J.; Pietryga, J. M.; Klimov, V. I. Apparent versus True Carrier Multiplication Yields in Semiconductor Nanocrystals. *Nano Lett.* **2010**, *10*, 2049−2057.
(31) Ip, A. H.; Thon, S. M.; Hoogland, S.; Voznyy, O.; Zhitomirsky, D.; Debnath, R.; Levina, L.; Rollny, L. R.; Carey, G. H.; Fischer, A.; et al. Hybrid Passivated Colloidal Quantum Dot Solids. *Nat. Nanotechnol.* **2012**, *7*, 577−582.
(32) Barkhouse, D. A. R.; Pattantyus-Abraham, A. G.; Levina, L.; Sargent, E. H. Thiols Passivate Recombination Centers in Colloidal Quantum Dots Leading to Enhanced Photovoltaic Device Efficiency. *ACS Nano* **2008**, *2*, 2356−2362.
(33) Konstantatos, G.; Levina, L.; Fischer, A.; Sargent, E. H. Engineering the Temporal Response of Photoconductive Photodetectors via Selective Introduction of Surface Trap States. *Nano Lett.* **2008**, *8*, 1446−1450.

(34) Nagpal, P.; Klimov, V. I. Role of Mid-gap States in Charge Transport and Photoconductivity in Semiconductor Nanocrystal Films. *Nat. Commun.* **2011**, *2*, 486.
(35) Castro, S. L.; Bailey, S. G.; Raffaelle, R. P.; Banger, K. K.; Hepp, A. F. Nanocrystalline Chalcopyrite Materials ($CuInS_2$ and $CuInSe_2$) via Low-Temperature Pyrolysis of Molecular Single-Source Precursors. *Chem. Mater.* **2003**, *15*, 3142−3147.
(36) Franzl, T.; Koktysh, D. S.; Klar, T. A.; Rogach, A. L.; Feldmann, J.; Gaponik, N. Fast Energy Transfer in Layer-By-Layer Assembled CdTe Nanocrystal Bilayers. *Appl. Phys. Lett.* **2004**, *84*, 2904−2906.
(37) Lazarenkova, O. L.; Balandin, A. A. Miniband Formation in a Quantum Dot Crystal. *J. Appl. Phys.* **2001**, *89*, 5509−5515.
(38) Trinh, M. T.; Limpens, R.; Boer, W. D. A. M.; de Schins, J. M.; Siebbeles, L. D. A.; Gregorkiewicz, T. Direct Generation of Multiple Excitons in Adjacent Silicon Nanocrystals Revealed by Induced Absorption. *Nat. Photonics* **2012**, *6*, 316−321.
(39) Tisdale, W. A.; Williams, K. J.; Timp, B. A.; Norris, D. J.; Aydil, E. S.; Zhu, X.-Y. Hot-Electron Transfer from Semiconductor Nanocrystals. *Science* **2010**, *328*, 1543−1547.
(40) Sandeep, C. S. S.; Cate, S.; ten Schins, J. M.; Savenije, T. J.; Liu, Y.; Law, M.; Kinge, S.; Houtepen, A. J.; Siebbeles, L. D. A. High Charge-Carrier Mobility Enables Exploitation of Carrier Multiplication in Quantum-Dot Films. *Nat. Commun.* **2013**, *4*, 2360.